

A reappraisal of constraints on Z' models from unitarity and direct searches at the LHC

Triparno Bandyopadhyay,^{a,*} Gautam Bhattacharyya,^{b,†} Dipankar Das,^{a,‡} Amitava Raychaudhuri^{a,§}

^a*Department of Physics, University of Calcutta, 92 Acharya Prafulla Chandra Road, Kolkata 700009, India*

^b*Saha Institute of Nuclear Physics, HBNI, 1/AF Bidhan Nagar, Kolkata 700064, India*

Abstract

We reexamine a minimal extension of the Standard Model (SM) through the introduction of an additional $U(1)$ symmetry leading to a new neutral gauge boson (Z'). An SM neutral scalar is used to spontaneously break this extra symmetry leading to the mass of the Z' . Except for three right-handed neutrinos no other fermions are added. After a brief recapitulation, we use the current LHC Drell-Yan (DY) data to put model independent constraints on the Z' couplings. Three important unknowns here are $M_{Z'}$, the Z - Z' mixing angle (α_z), and the extra $U(1)$ gauge coupling (g_x). Treating g_x as a parameter, juxtaposition of additional constraints from unitarity and low energy neutrino-electron scattering on that obtained from the direct searches allows us to extract the following limits in the gauged $(B - L)$ model: $M_{Z'} > 3.5$ TeV and $|\alpha_z| < 0.003$, when the strength of the additional $U(1)$ gauge coupling is the same as that of the SM $SU(2)_L$. For vanishing Z - Z' mixing, the lower limit on $M_{Z'}$ goes up to 4 TeV. For some other $U(1)$ models we considered, the bounds turn out to be roughly of the same order.

1 Introduction

Of all the Beyond Standard Model (BSM) scenarios, none is more ubiquitous than models with an extra $U(1)$ symmetry in addition to the SM symmetry, giving a neutral spin-1 massive gauge boson, Z' . Its theoretical motivation comes from various directions. Left-right symmetric models, Grand Unified Theories (GUT) larger than $SU(5)$, e.g. $SO(10)$ or E_6 , as well as string models, all entail an extra gauged $U(1)$ in addition to the SM group [1–14]. Non-supersymmetric BSM scenarios, advocated to address the hierarchy problem, such as Little Higgs models [15, 16] with extended gauge sectors contain $U(1)$ as an extra gauge group. Even dynamical supersymmetry breaking triggered by an anomalous $U(1)$ has been extensively discussed (for a review, see [17]). Leaking of the standard Z boson into an extra dimension yields, from a 4d perspective, an infinite tower of increasingly more massive Kaluza-Klein modes, each such mode resembling a Z' boson of a gauged $U(1)$ carrying specific symmetries [18–20]. Besides, a Z' model with a gauged $(B - L)$ symmetry has been used to address the hierarchy problem by facilitating electroweak symmetry breaking radiatively *à la* Coleman-Weinberg keeping classical conformal invariance and stability up to the Planck scale [21]. Cosmological inflation scenarios with non-minimal gravitational coupling have been studied in a similar context where the inflaton coupling is correlated to the Z' coupling [22]. $U(1)$ gauge bosons also constitute important ingredients in cosmic string models [23].

On the other hand, Z' has been fruitfully employed in many theoretically well-motivated models as a portal to dark matter (DM), mediating between the dark sector and the visible sector [24–26]. The DM itself could be a $U(1)$ gauge boson of the dark sector. A heavy Z' in such models could be realized in a gauge invariant way by the Stückelberg mechanism [27]. In the astrophysical context too a Z' gauge boson has been advocated to account for the γ -ray excess in the galactic center [28, 29].

*gondogolegogol@gmail.com

†gautam.bhattacharyya@saha.ac.in

‡ddphy@caluniv.ac.in

§palitprof@gmail.com

Thus there is enough motivation for the Z' mass and coupling to be an important part of phenomenological studies in the context of colliders [10, 30–35], the collider-dark matter interface [36–39], flavor physics [40, 41] and electroweak precision tests [42–44]. In this work we use the latest ATLAS (LHC) Drell-Yan data (36 fb^{-1} luminosity) to set model-independent bounds on the fermionic couplings of Z' . For this we use the data for both $(e^+e^-, \mu^+\mu^-)$ as well as the $\tau^+\tau^-$ final states. In addition, we use s-wave unitarity to set upper bounds on $M_{Z'}$ as a function of the Z - Z' mixing angle (α_z). Together with these two, we use the low energy ν_μ - e scattering data to set strong constraints in the parameter space defined by $M_{Z'}$, α_z , and g'_x , the effective gauge coupling of the additional $U(1)$ taking into account the scope for kinetic mixing, for several anomaly-free extensions of the SM.

Very recently, constraints directly on $M_{Z'}$ for various $U(1)$ extensions have been derived in [45] using the 36 fb^{-1} ATLAS data, and wherever we overlap we roughly agree with their limits. Constraints directly on $M_{Z'}$ were also obtained in [46] assuming that the Z - Z' mixing angle is small, but those limits are obviously a bit weaker as they were extracted using the then available ATLAS data with much lower luminosity.

Our paper is organized as follows. In Sec. 2, we set up our notations recapitulating the Z' -extension of the SM touching upon the scalar and the fermion sectors. Then, in Sec. 3, we use the latest 36 fb^{-1} ATLAS Drell-Yan (DY) data [47, 48] to set constraints on the fermion couplings of the Z' in a model independent manner. Next, in Sec. 4, we discuss the bounds on the Z' -mass and the Z - Z' mixing angle arising from s-wave unitarity. Note that this bound depends only on $M_{Z'}$ and the Z - Z' mixing angle and is independent of the Z' couplings to the fermions. Once those fermionic couplings are chosen, a bound on the same plane arises from the low energy ν_μ - e scattering data, which we discuss in Sec. 5. In Sec. 6, we combine the limits arising from these different aspects to identify the region currently allowed for different $U(1)$ extensions. We end with our conclusions where we highlight the novel features of our analysis.

2 Minimal Z' model – a small recapitulation

As noted in the introduction, BSM scenarios with an electrically neutral, massive vector-boson, Z' , are quite common in the literature. The simplest realizations of Z' models are the ones where the SM gauge symmetry, $\mathcal{G}_{\text{SM}} \equiv SU(3)_C \otimes SU(2)_L \otimes U(1)_Y$, is minimally extended to $\mathcal{G}_{\text{SM}} \otimes U(1)_X$. The $U(1)_X$ is broken by a \mathcal{G}_{SM} singlet scalar, S , charged under $U(1)_X$. We choose this charge to be $1/2$, which fixes the convention for g_x – the gauge coupling corresponding to $U(1)_X$. Thus, in the minimalistic scenario, we have the following scalar fields:

$$\Phi \equiv (1, 2, 1/2, x_\Phi/2); \quad S \equiv (1, 1, 0, 1/2), \quad (1)$$

where Φ denotes the usual $SU(2)_L$ doublet responsible for the SM gauge symmetry breaking as well as the Dirac masses of fermions. The quantities inside the parentheses characterize the transformation properties under the gauge group $SU(3)_C \otimes SU(2)_L \otimes U(1)_Y \otimes U(1)_X$. The electric charge is given by:

$$Q = T_{3L} + Y, \quad (2)$$

where T_{3L} and Y are the third component of weak isospin and the hypercharge respectively. As Φ transforms in a nontrivial manner under $SU(2)_L$, $U(1)_Y$, and $U(1)_X$ there will be mixing among the neutral gauge boson states when Φ develops a vacuum expectation value (vev). The mass eigenstates which emerge will be identified as the massless photon (A), the SM Z , and an exotic Z' . Note that even if we start with $x_\Phi = 0$, Φ can develop a $U(1)_X$ charge due to gauge-kinetic mixing among the two abelian field strength tensors [49]. Also, in general, there will be mixing among the neutral scalars coming from Φ and S , and a certain composition of the two should correspond to the SM-like scalar observed at the LHC.

Abelian extensions of the SM are typically motivated by some high scale physics related to an elaborate scalar sector, and it might seem that the two-scalar mixing scenario we are considering here is a bit too simplistic. However, we are interested in models where the new physics beyond the extra $U(1)_X$ is at too high a scale to have any meaningful contribution to $\mathcal{O}(\text{TeV})$ physics, or too weakly coupled. With that in mind, such a minimal framework is capable of describing the gauge-scalar sector of a wide array of $U(1)$ extensions of the SM, which are differentiated by the fermionic charges under the $U(1)_X$. In the following sub-sections, we describe our framework in detail, starting with the scalar potential. In passing, it should be noted that in the literature, one is often faced with models where the extended gauge symmetry is given by $SU(3)_C \otimes SU(2)_L \otimes U(1)_1 \otimes U(1)_2$, where the SM $U(1)_Y$ is a linear combination of $U(1)_1$ and $U(1)_2$. An example is the $U(1)_R \otimes U(1)_{B-L}$, of left-right symmetric models. In such cases, we can always perform a rotation in the $U(1)$ generators plane to get the $U(1)_Y \otimes U(1)_X$ basis that we are using.

2.1 The gauge-scalar sector

The gauge-scalar part of the Lagrangian for minimal $\mathcal{G}_{\text{SM}} \otimes U(1)_X$ models is given by:

$$\mathcal{L} = \mathcal{L}_{\text{GK}} + \mathcal{L}_{\text{SK}} - V(\Phi, S), \quad (3)$$

where \mathcal{L}_{GK} and \mathcal{L}_{SK} are the kinetic Lagrangians in the gauge and the scalar sectors respectively and $V(\Phi, S)$ denotes the scalar potential, expressions for which appear below:

$$\mathcal{L}_{\text{GK}} = -\frac{1}{4}W_{\mu\nu}^a W_a^{\mu\nu} - \frac{1}{4}B_{\mu\nu}B^{\mu\nu} - \frac{1}{4}X_{\mu\nu}X^{\mu\nu} - \frac{\sin\chi}{2}B_{\mu\nu}X^{\mu\nu}, \quad (4a)$$

$$\mathcal{L}_{\text{SK}} = (D^\mu\Phi)^\dagger(D_\mu\Phi) + (D^\mu S)^\dagger(D_\mu S), \quad (4b)$$

$$V(\Phi, S) = -\mu^2(\Phi^\dagger\Phi) - \mu_S^2(S^\dagger S) + \lambda_\Phi(\Phi^\dagger\Phi)^2 + \lambda_S(S^\dagger S)^2 + \lambda_{\Phi S}(\Phi^\dagger\Phi)(S^\dagger S). \quad (4c)$$

In the equation above, $W_{\mu\nu}^a$, $B_{\mu\nu}$, and $X_{\mu\nu}$ denote the field tensors corresponding to $SU(2)_L$, $U(1)_Y$, and $U(1)_X$ respectively, and the covariant derivatives for Φ and S are given by:

$$D_\mu\Phi = \left(\partial_\mu - ig\frac{\tau_a}{2}W_\mu^a - i\frac{g_Y}{2}B_\mu - i\frac{g_X}{2}x_\Phi X_\mu\right)\Phi, \quad (5a)$$

$$D_\mu S = \left(\partial_\mu - i\frac{g_X}{2}X_\mu\right)S. \quad (5b)$$

In the equation above τ_a represents the Pauli matrices and the naming convention of the gauge fields mirrors that of the field strength tensors.

Note that, in the $(B^{\mu\nu}, X^{\mu\nu})$ basis, \mathcal{L}_{GK} contains the gauge kinetic mixing term $(\sin\chi/2)B^{\mu\nu}X_{\mu\nu}$ [49]. We can perform a general linear transformation to go to a basis where \mathcal{L}_{GK} is canonically diagonal [50, 51]:

$$\begin{pmatrix} B_\mu \\ X_\mu \end{pmatrix} \rightarrow \begin{pmatrix} B'_\mu \\ X'_\mu \end{pmatrix} = \begin{pmatrix} 1 & \sin\chi \\ 0 & \cos\chi \end{pmatrix} \begin{pmatrix} B_\mu \\ X_\mu \end{pmatrix}. \quad (6)$$

In this basis, the gauge-kinetic Lagrangian becomes:

$$\mathcal{L}_{\text{GK}} = -\frac{1}{4}W_{\mu\nu}^a W_a^{\mu\nu} - \frac{1}{4}B'_{\mu\nu}B'^{\mu\nu} - \frac{1}{4}X'_{\mu\nu}X'^{\mu\nu}, \quad (7)$$

and the covariant derivatives take the following forms:

$$D_\mu\Phi = \partial_\mu\Phi - i\frac{g}{2}(\tau_a W_\mu^a + \tan\theta_w B_\mu + \tan\theta_x x'_\Phi X'_\mu)\Phi, \quad (8a)$$

$$D_\mu S = \left(\partial_\mu - i\frac{g'_x}{2}X'_\mu\right)S, \quad (8b)$$

where we have defined,

$$\tan\theta_w = \frac{g_Y}{g}, \quad (9a)$$

$$\tan\theta_x = \frac{g'_x}{g}, \quad (9b)$$

$$\text{with } g'_x = g_x \sec\chi, \quad (9c)$$

$$\text{and } x'_\Phi = x_\Phi - \frac{g_Y}{g_x} \sin\chi. \quad (9d)$$

Eqs. (9c) and (9d) reflect how the definitions of the gauge coupling and the gauge charge of Φ corresponding to the extra $U(1)$ will be modified in the presence of gauge kinetic mixing. In the limit of zero kinetic mixing, $\tan\theta_x$ characterizes the strength of the $U(1)_X$ gauge coupling relative to the weak gauge coupling.

After spontaneous symmetry breaking (SSB), we expand the scalar fields, in the unitary gauge, as

$$\Phi = \frac{1}{\sqrt{2}} \begin{pmatrix} 0 \\ v + \phi_0 \end{pmatrix}, \quad S = \frac{1}{\sqrt{2}}(v_s + s), \quad (10)$$

where v and v_s are the vevs for Φ and S respectively. This will lead to the neutral gauge boson mass matrix, in the basis where the gauge kinetic terms are diagonal, which can be written as follows:

$$\mathcal{L}_N^{\text{mass}} = \frac{1}{2} \begin{pmatrix} W_\mu^3 & B'_\mu & X'_\mu \end{pmatrix} \cdot \mathcal{M}_N^2 \cdot \begin{pmatrix} W_\mu^3 \\ B'_\mu \\ X'_\mu \end{pmatrix}, \quad (11)$$

where

$$\mathcal{M}_N^2 = \frac{g^2 v^2}{4} \begin{pmatrix} 1 & -\tan \theta_w & -x'_\Phi \tan \theta_x \\ -\tan \theta_w & \tan^2 \theta_w & x'_\Phi \tan \theta_x \tan \theta_w \\ -x'_\Phi \tan \theta_x & x'_\Phi \tan \theta_x \tan \theta_w & \tan^2 \theta_x (r^2 + x_\Phi'^2) \end{pmatrix}, \quad (12)$$

with $r = v_s/v$. The mass matrix in Eq. (12) can be block diagonalized as follows:

$$O_w^T \cdot \mathcal{M}_N^2 \cdot O_w = \frac{g^2 v^2}{4} \begin{pmatrix} 0 & 0 & 0 \\ 0 & \sec^2 \theta_w & -x'_\phi \tan \theta_x \sec \theta_w \\ 0 & -x'_\phi \tan \theta_x \sec \theta_w & \tan^2 \theta_x (r^2 + x_\phi'^2) \end{pmatrix}, \quad (13)$$

where

$$O_w = \begin{pmatrix} \sin \theta_w & \cos \theta_w & 0 \\ \cos \theta_w & -\sin \theta_w & 0 \\ 0 & 0 & 1 \end{pmatrix}. \quad (14)$$

The massless photon, A_μ , is then readily extracted as

$$\begin{pmatrix} A_\mu \\ Z_{1\mu} \\ X'_\mu \end{pmatrix} = O_w^T \begin{pmatrix} W_\mu^3 \\ B'_\mu \\ X'_\mu \end{pmatrix}. \quad (15)$$

Diagonalization of the remaining 2×2 block of the matrix in Eq. (13), gives rise to the remaining mass eigenstates, namely, Z and Z' . The rotation between the gauge, and the mass bases is given by:

$$\begin{pmatrix} B'_\mu \\ W_\mu^3 \\ X'_\mu \end{pmatrix} = \begin{pmatrix} \cos \theta_w & -\sin \theta_w \cos \alpha_z & \sin \theta_w \sin \alpha_z \\ \sin \theta_w & \cos \theta_w \cos \alpha_z & -\cos \theta_w \sin \alpha_z \\ 0 & \sin \alpha_z & \cos \alpha_z \end{pmatrix} \begin{pmatrix} A_\mu \\ Z_\mu \\ Z'_\mu \end{pmatrix}. \quad (16)$$

This second step of diagonalization then entails the following relations:

$$M_{11}^2 \equiv M_Z^2 \cos^2 \alpha_z + M_{Z'}^2 \sin^2 \alpha_z = \frac{M_W^2}{\cos^2 \theta_w}, \quad (17a)$$

$$M_{Z'}^2 \cos^2 \alpha_z + M_Z^2 \sin^2 \alpha_z = M_W^2 \tan^2 \theta_x (r^2 + x_\phi'^2), \quad (17b)$$

$$(M_{Z'}^2 - M_Z^2) \sin(2\alpha_z) = \frac{2x'_\phi \tan \theta_x M_W^2}{\cos \theta_w}, \quad (17c)$$

where $M_W = gv/2$ denotes the W -boson mass. While the gauge-scalar sector described here holds generally for minimal Z' models, the fermion charge assignments vary across them. However, a general formalism can be developed for the fermionic sector as well, which we discuss the next subsection.

2.2 Anomaly cancellation and fermionic charge assignments

In this work we look at the models in which the fermion sector of the SM is extended by a right-handed (RH) neutrino, N_i , per generation. We are interested in the situation where the RH neutrinos get Majorana masses from their Yukawa interactions with S . Under the assumption of generation universality, the possible $U(1)_X$ charge options for the fermions are quite restricted, as we now discuss.

We assign a $U(1)_X$ charge x_q for the left-handed quark doublets and x_l for the left-handed lepton doublets. For the right-handed u -type (d -type) quarks we assign the charges x_u (x_d) while for the right-handed electron we take it to be x_e . The x -charge of the right-handed neutrinos, N , is taken as x_N . The x quantum numbers of the scalars have already been introduced: the SM Higgs doublet, Φ , has a charge $x_\Phi/2$, while S has a charge $1/2$.

Since the scalar Φ is responsible for the fermion Dirac masses, we must have

$$x_q - x_u = x_e - x_l = x_d - x_q = -\frac{x_\Phi}{2}. \quad (18)$$

In addition, since S is assumed to be responsible for the Majorana masses of the right-handed neutrinos, x_N can be determined as

$$x_N = -1/4. \quad (19)$$

Further, demanding cancellation of gauge and gravitational anomalies, we get

$$[SU(2)_L]^2 U(1)_X \Rightarrow 3x_q + x_l = 0, \quad (20a)$$

$$[SU(3)_C]^2 U(1)_X \Rightarrow 2x_q = x_d + x_u, \quad (20b)$$

$$[U(1)_Y]^2 U(1)_X \Rightarrow 2x_q + 6x_l = 16x_u + 4x_d + 12x_e, \quad (20c)$$

$$\text{Gauge Gravity} \Rightarrow 6x_q + 2x_l = 3(x_u + x_d) + (x_e + x_N). \quad (20d)$$

It can be checked that the other two constraints that follow from the $U(1)_Y[U(1)_X]^2$ and $[U(1)_X]^3$ triangle anomalies are automatically satisfied. Eq. (20) contains four relations among the six unknowns x_q, x_l, x_u, x_d, x_e , and x_N . Taken together with Eq. (18) and bearing in mind that x_N is fixed from eq. Eq. (19), all the x charges of the fermions can be determined in terms of one free parameter¹, κ_x , as depicted in Table 1.

Multiplet	$SU(3)_C$	$SU(2)_L$	$U(1)_Y$	$U(1)_X$
Q_L	3	2	1/6	$\kappa_x/3$
u_R	3	1	2/3	$4\kappa_x/3 - 1/4$
d_R	3	1	-1/3	$-2\kappa_x/3 + 1/4$
L_L	1	2	-1/2	$-\kappa_x$
e_R	1	1	-1	$-2\kappa_x + 1/4$
N_R	1	1	0	$-1/4$
Φ	1	2	1/2	$\kappa_x - 1/4$
S	1	1	0	$1/2$

Table 1: The $U(1)_X$ -charge assignment and the other quantum numbers of the fermions and scalars satisfying the anomaly constraints.

Different $U(1)_X$ models are obtained by choosing κ_x appropriately. In Table 2 we have shown several alternatives. For example, the $(B - L)$ extension of the SM corresponds to $\kappa_x = \frac{1}{4}$. For this choice the x charges are precisely $(B - L)/4$ – the overall factor of $1/4$ being a reflection of our chosen normalization of the $U(1)_X$ coupling constant, g_x . It is worth noting that for this choice of κ the $SU(2)_L$ doublet scalar Φ has $U(1)_X$ charge $x_\Phi/2 = 0$. Hence, the Z - Z' mixing in $B - L$ models is strictly due to gauge kinetic mixing, which imparts a $U(1)_X$ charge onto Φ . The choice, $\kappa_x = 0$ corresponds to the case where $U(1)_X \equiv U(1)_R$ under which the left-handed fermions are singlets while right-handed fermions have charges $\pm 1/4$. Choosing $\kappa_x = \frac{3}{20}$ gives $U(1)_X \equiv U(1)_\chi$ which emerges when an $SO(10)$ GUT is broken to $SU(5) \times U(1)_\chi$. Finally, with $\kappa_x = \frac{1}{5}$ we get the $U(1)_R \times U(1)_{B-L}$ model which can be rotated to the $U(1)_Y \times U(1)_X$ form with the $U(1)_X$ charge satisfying $4x = \frac{3}{5}T_3 - \frac{2}{5}(B - L)$. In Table 2 we have also summarized how the usually normalized $U(1)$ charges in these models are related to the $U(1)_X$ charges given in the last column of Table 1.

Model	$U(1)_{B-L}$	$U(1)_R$	$U(1)_\chi$	$U(1)_R \times U(1)_{B-L}$
Charge	$\frac{(B-L)}{4}$	$\frac{T_{3R}}{2}$	$-Q_\chi/\sqrt{10}$	$\frac{1}{4} \left\{ \frac{3}{5}T_{3R} - \frac{2}{5}(B - L) \right\}$
κ_x	$\frac{1}{4}$	0	$\frac{1}{4} \cdot \frac{3}{5}$	$\frac{1}{4} \cdot \frac{4}{5}$

Table 2: κ_x for different $U(1)_X$ models. Note that for the $B - L$ model, our $U(1)_{B-L}$ charge differs from the conventional choice by a factor of $1/4$ due to our convention for the gauge coupling of the additional $U(1)_X$.

2.3 Fermion couplings to gauge bosons

The parametrization for fermion charges being set, we can now write down the fermion couplings to Z and Z' , which will be necessary for the subsequent discussions. The relevant interaction Lagrangian can be written, in the κ_x formalism, as:

$$\mathcal{L}_{\text{int}} = -\frac{g}{2 \cos \theta_w} \left[\bar{f} \gamma^\mu \left(g_V^f - g_A^f \gamma^5 \right) f Z_\mu + \bar{f} \gamma^\mu \left(g_V^{f'} - g_A^{f'} \gamma^5 \right) f Z'_\mu \right], \quad (21)$$

¹Ref. [46] also introduces a parametrization for the Z' fermionic charges, but our formulation is slightly different.

where f stands for a generic fermion. Our interest later in Sec. 5 will be on the couplings of specifically neutrinos and the charged leptons. So, in the following we give explicit expressions for the cases with $f = \nu$ and $f = e$, though the generalization to other fermions is straightforward.

For the left-handed neutrinos we define $\kappa_{Z, Z'}$ through

$$g_V^\nu = g_A^\nu = \frac{\kappa_Z}{2}, \quad g_V^{\nu'} = g_A^{\nu'} = \frac{\kappa_{Z'}}{2}. \quad (22)$$

Using the results of Sec. 2.1 and 2.2 we get:

$$\kappa_Z = \cos \alpha_z - \sin \alpha_z \left[\left(3\kappa_x - \frac{1}{4} \right) \frac{M_W}{M_{11}} \tan \theta_x + \mathcal{F} \right], \quad (23a)$$

$$\kappa_{Z'} = -\sin \alpha_z - \cos \alpha_z \left[\left(3\kappa_x - \frac{1}{4} \right) \frac{M_W}{M_{11}} \tan \theta_x + \mathcal{F} \right], \quad (23b)$$

$$g_V^e = \cos \alpha_z \left(\frac{3}{2} - \frac{2M_W^2}{M_{11}^2} \right) - \sin \alpha_z \left[\left(\frac{9\kappa_x}{2} - \frac{5}{8} \right) \frac{M_W}{M_{11}} \tan \theta_x + \frac{3}{2} \mathcal{F} \right], \quad (23c)$$

$$g_V^{e'} = -\sin \alpha_z \left(\frac{3}{2} - \frac{2M_W^2}{M_{11}^2} \right) - \cos \alpha_z \left[\left(\frac{9\kappa_x}{2} - \frac{5}{8} \right) \frac{M_W}{M_{11}} \tan \theta_x + \frac{3}{2} \mathcal{F} \right], \quad (23d)$$

$$g_A^e = -\frac{1}{2} \cos \alpha_z + \sin \alpha_z \left[\left(\frac{3\kappa_x}{2} - \frac{3}{8} \right) \frac{M_W}{M_{11}} \tan \theta_x + \frac{\mathcal{F}}{2} \right], \quad (23e)$$

$$g_A^{e'} = \frac{1}{2} \sin \alpha_z + \cos \alpha_z \left[\left(\frac{3\kappa_x}{2} - \frac{3}{8} \right) \frac{M_W}{M_{11}} \tan \theta_x + \frac{\mathcal{F}}{2} \right], \quad (23f)$$

where the expression for \mathcal{F} is given by

$$\mathcal{F} = \frac{(M_{Z'}^2 - M_Z^2)}{M_{11}^2} \sin \alpha_z \cos \alpha_z. \quad (24)$$

In the subsequent sections we will use these expressions to put constraints on different Z' -models.

3 Bounds from direct searches at the LHC

The LHC experiments CMS and ATLAS routinely search for exotic neutral vector resonances going to $\ell^+ \ell^-$ ($\ell \equiv e, \mu, \tau$) final states. The non-discovery of any such new particle till date translates to exclusion limits on the mass and couplings of the Z' . In this section we extract such bounds using the latest 36 fb^{-1} ATLAS data [47], and cast them in a model independent manner.

To analyse the constraints arising from direct resonant Z' production at the LHC, decaying to a pair of charged leptons, we first define the chiral couplings g_L^f and g_R^f through:

$$g_R^f = \frac{g}{2 \cos \theta_W} (g_V^{f'} - g_A^{f'}), \quad g_L^f = \frac{g}{2 \cos \theta_W} (g_V^{f'} + g_A^{f'}). \quad (25)$$

From Eq. (22) we note that the right-handed couplings of the light neutrinos to Z' , $g_R^{\nu'}$, are zero. In writing Eq. (25), we have implicitly assumed flavor diagonal couplings for Z' , but kept open the possibility of flavor nonuniversality. With this, the cross section for resonant production of a Z' boson at the LHC and its subsequent decay into a pair of charged leptons, in the narrow width approximation, can be conveniently expressed as [30]:²

$$\sigma(pp \rightarrow Z' X \rightarrow \ell^+ \ell^- X) = \frac{\pi}{6s} \sum_q C_q^\ell w_q(s, M_{Z'}^2), \quad (26)$$

where the sum is over all the partons. The co-efficients,

$$C_q^\ell = \left[(g_L^\ell)^2 + (g_R^\ell)^2 \right] \text{BR}(Z' \rightarrow \ell^+ \ell^-) \quad (27)$$

involve the fermionic couplings of Z' and hence depend on the details of the fermionic sector of the model under consideration. The functions w_q , on the other hand, contain all the information about the parton distribution

²The reader may note a difference of a $1/8$ factor between our expression and the one given in Ref. [30]. This issue has been addressed in Refs. [52, 53] whose conventions we follow here.

functions (PDFs) and QCD corrections, detailed expressions for which appear in the Appendix. Considering the fact that w_u and w_d are substantially larger than the w_q functions for the other quarks, we can approximate Eq. (26) as follows³:

$$\sigma(pp \rightarrow Z'X \rightarrow \ell^+\ell^-X) \approx \frac{\pi}{6s} [C_u^\ell w_u(s, M_{Z'}^2) + C_d^\ell w_d(s, M_{Z'}^2)]. \quad (28)$$

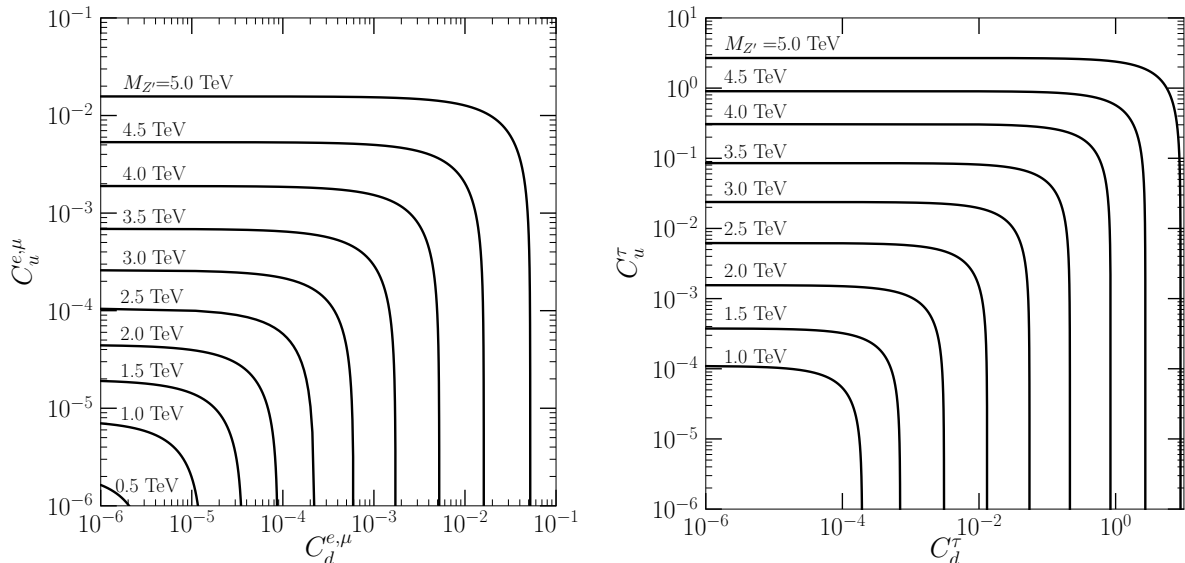


Figure 1: *Exclusion contours at 95% C.L. in the C_u^ℓ - C_d^ℓ plane for different values of $M_{Z'}$, derived using ATLAS data for dilepton final states [47,48]. In the left panel the contours are for the $\ell \equiv e, \mu$ final state, and the right panel corresponds to the $\tau^+\tau^-$ final state. For any given $M_{Z'}$, the interior of the corresponding contour is allowed.*

Direct searches at the LHC put upper limits on the left-hand-side of Eq. (26). The most recent ATLAS limits can be found in [47,48] where, as expected, the bound for the $\ell^\pm \equiv \tau^\pm$ case is less stringent than for $\ell^\pm \equiv e^\pm, \mu^\pm$. Using the CT14NNLO PDF set [55], we evaluate w_u and w_d , and translate the limit on the cross section into a bound in the C_u^ℓ - C_d^ℓ plane for different values of $M_{Z'}$. The results have been displayed in Fig. 1, where the left panel corresponds to $\ell \equiv e, \mu$,⁴ and the right panel corresponds to $\ell \equiv \tau$. For any chosen $M_{Z'}$, only the interior of the corresponding contour is allowed. Although the bound arising from the $\tau^+\tau^-$ final state is substantially weaker compared to the $e^+e^-, \mu^+\mu^-$ final state, it may hold situational merits for scenarios where, *e.g.*, the Z' dominantly couples to the third generation of fermions [57–59].

4 Theoretical constraint from unitarity

For minimal $U(1)_X$ models, it is well known that in the absence of Z' the scattering amplitude for the process $W_L^+W_L^- \rightarrow W_L^+W_L^-$, where W_L^\pm denotes the longitudinal component of the W -boson, will grow as the fourth power of the CoM energy at the leading order. To put it explicitly, if the Z' is too heavy to contribute, then we can write the Feynman amplitude for $W_L^+W_L^- \rightarrow W_L^+W_L^-$ as

$$\mathcal{M}_{W_L^+W_L^- \rightarrow W_L^+W_L^-} = \frac{g^2 \cos^2 \theta_w E^4}{M_W^4} \sin^2 \alpha_z (-3 + 6 \cos \theta + \cos^2 \theta) + \mathcal{O}\left(\frac{E^2}{M_{Z'}^2}\right), \quad (29)$$

where E denotes the CoM energy and θ is the scattering angle. From Eq. (29), the $l = 0$ partial wave amplitude which usually gives the strongest bound, can be extracted as

$$a_0 = -\frac{8}{3} \frac{g^2 \cos^2 \theta_w E^4}{M_W^4} \sin^2 \alpha_z. \quad (30)$$

³For most Z' models this is a reasonable approximation. In particular, in models with flavor universal Z' couplings we have checked that it hardly makes a visible difference if we use Eq. (26) instead of the approximate formula of Eq. (28). But, of course, this approximation breaks down in the extreme case when the Z' does not couple at all to the first generation of quarks [54].

⁴Such an analysis was carried out by CMS using their 8 TeV (20 fb⁻¹) dilepton data [56]. A comparison with our results shows that there is almost an order of magnitude improvement in the corresponding bounds, if we use the current 13 TeV (36 fb⁻¹) data.

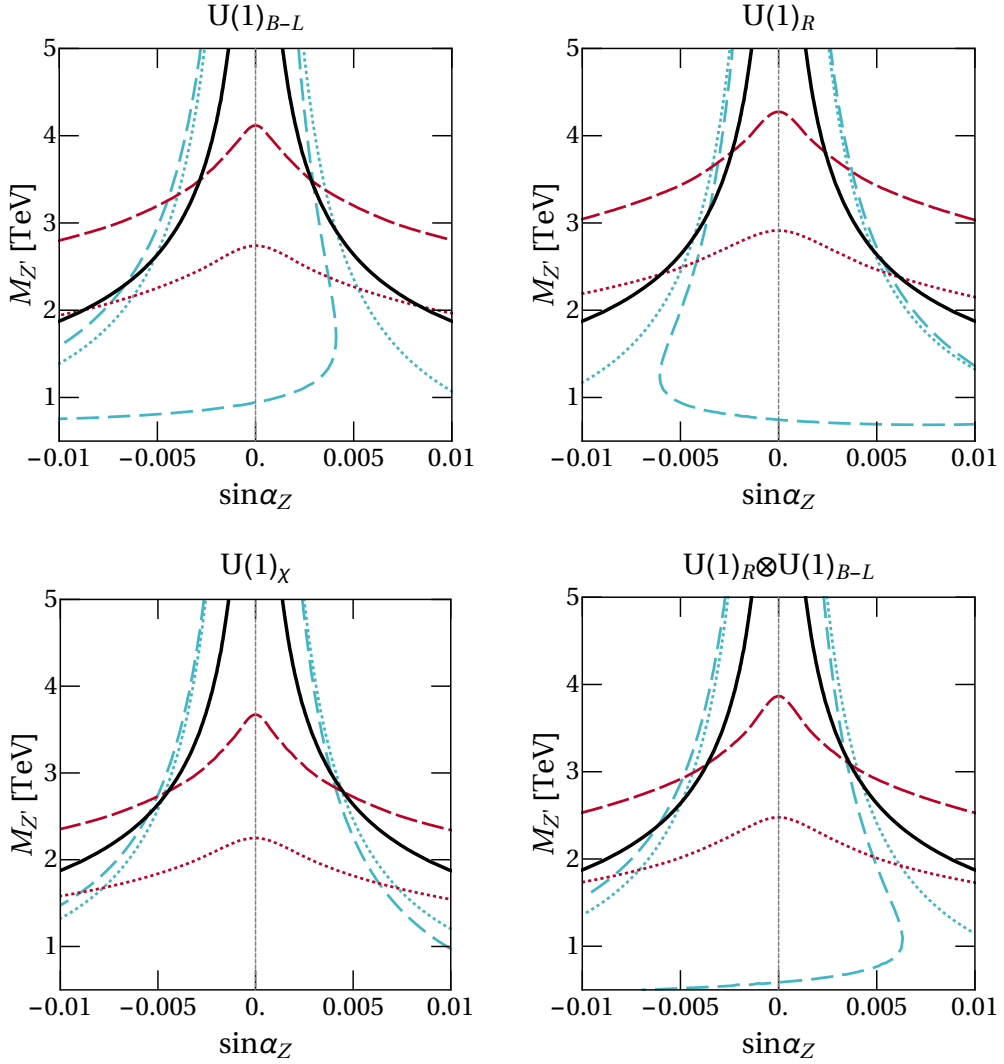


Figure 2: Bounds in the $M_{Z'}$ - $\sin \alpha_z$ plane for the four models listed in Table 2. In every panel, the region contained within the two solid black lines is allowed from unitarity. The dark red and the light blue colors indicate the limits set by direct detection and ν_μ - e scattering data, respectively. The dotted and dashed line types correspond to $\tan \theta_x = 4$ and 1, respectively. Regions above the dark red lines are allowed by the 36 fb^{-1} ATLAS data whereas the interiors of the light blue contours represent the allowed area from the ν_μ - e scattering data.

Unitarity restricts the magnitude of a_0 as $|a_0| < 8\pi$ which translates into an upper bound for the CoM energy,

$$E < E_{\max} = \left[8\pi \times \frac{3(M_Z^2 \cos^2 \alpha_z + M_{Z'}^2 \sin^2 \alpha_z)}{32\sqrt{2}G_F \sin^2 \alpha_z} \right]^{\frac{1}{4}}, \quad (31)$$

where G_F is the Fermi constant obtained via the relation,

$$g^2/M_W^2 = 4\sqrt{2}G_F, \quad (32)$$

and we have used Eq. (17a) to substitute for $M_W^2/\cos^2 \theta_w$. Thus, to restore unitarity, effects of the Z' must set in before the CoM energy reaches E_{\max} , i.e., $M_{Z'} < E_{\max}$ which implies:

$$\frac{M_{Z'}^4 \sin^2 \alpha_z}{(M_Z^2 \cos^2 \alpha_z + M_{Z'}^2 \sin^2 \alpha_z)} < 8\pi \times \frac{3}{32\sqrt{2}G_F}. \quad (33)$$

The tree unitarity constraint is of prime importance as it translates to an upper bound on $M_{Z'}$, for a given $\sin \alpha_z$, as can be seen from Eq. (33)⁵. We show this explicitly when we discuss the interplay of the different

⁵Similarly for $f\bar{f} \rightarrow W_L^+ W_L^-$ the scattering amplitude will grow as $\mathcal{O}(E^2)$ [60] and can give an upper bound on $M_{Z'}$ for nonzero α_z . But this bound will depend on the fermionic couplings of Z' [61] and will not be as model independent.

bounds, in Sec. 6. It should also be noted that although unitarity in the context of Z' models have been studied earlier [62], to our knowledge, the possibility of using it to cast an upper bound on the Z' mass as in Eq. (33) has not been emphasized before and constitutes a new observation in our paper. Moreover, since this analysis does not depend on the fermionic details of the model, such a bound is quite general and can be applied to a vast variety of Z' models.

5 Constraints from ν_μ - e scattering

The unitarity constraint described in the previous section, relies on sniffing the effects of Z' through the Z - Z' mixing. Therefore the bounds are lifted in the limit $\sin \alpha_z = 0$ as has been clearly depicted in Fig. 2. However, depending on how Z' couples to the fermions, it is possible to put lower bounds on $M_{Z'}$, even in the limit of vanishing Z - Z' mixing [63, 64]. This can be done, *e.g.*, by using the data from low energy neutrino-electron scattering such as $\nu_\mu e \rightarrow \nu_\mu e$ which proceeds, at the tree level, purely via neutral current. In models with an extra $U(1)$, the Z' boson will, in general, also contribute to the scattering.

The dimension-six operator governing $\nu_\mu e$ scattering at low energies is written as:

$$\mathcal{L}_{\nu e} = -\frac{G_F}{\sqrt{2}} [\bar{\nu}\gamma^\mu (1 - \gamma^5) \nu] [\bar{e}\gamma_\mu (g_V^{\nu e} - g_A^{\nu e}\gamma^5) e]. \quad (34)$$

We recall that in the SM, the expressions for $g_V^{\nu e}$ and $g_A^{\nu e}$ are very simple at the tree level and are given by

$$(g_V^{\nu e})^{\text{SM}} \equiv (g_V^e)^{\text{SM}} = -\frac{1}{2} + 2\sin^2 \theta_w, \quad (g_A^{\nu e})^{\text{SM}} \equiv (g_A^e)^{\text{SM}} = -\frac{1}{2}. \quad (35)$$

Of course, in the minimal Z' models, the above expressions will be modified as follows:

$$(g_{(V,A)}^{\nu e})^{\text{model}} = M_{11}^2 \left(\frac{\kappa_Z g_{(V,A)}^e}{M_Z^2} + \frac{\kappa_{Z'} g_{(V,A)}^{\prime e}}{M_{Z'}^2} \right), \quad (36)$$

where the expression for M_{11}^2 appears in Eq. (17a) and the rest of the couplings in Eq. (23).

We use this formula along with the following data from PDG [65]

$$g_V^{\nu e} = -0.040 \pm 0.015, \quad g_A^{\nu e} = -0.507 \pm 0.014, \quad (37)$$

to draw the 1σ allowed regions in the $\sin \alpha_z$ - $M_{Z'}$ plane for two different values of $\tan \theta_x$ as shown by the blue curves in Figs. 2 and 3.

6 Results and discussions

Till now we have developed a general formalism on how to constrain a minimal Z' model from theoretical considerations as well as experimental data. Once a specific model is chosen, κ_x (in Table 1) assumes a definite value, and the different limits described in the previous sections can be combined together to give stronger bounds on the parameter space. To illustrate, for the four models listed in Table 2, $C_{u,d}^{e,\mu}$ and $g_V^{\nu e}$ ⁶ can be determined, using Eqs. (27), (25) and (36) in conjunction with Eq. (23), in terms of the model parameters $M_{Z'}$, α_z and $\tan \theta_x$. The bound from the left panel of Fig. 1 and the constraint coming from ν_μ - e scattering can then be translated, in terms of these parameters, for specific models. In the four panels of Fig. 2 these bounds have been displayed in the $M_{Z'}$ - $\sin \alpha_z$ plane for the four $U(1)_X$ models, for different values of $\tan \theta_x$. The figures have been appropriately labeled in accordance with the model they represent. The upper bound on $M_{Z'}$ from unitarity, represented by the solid black line, is the same for all four models, and is also independent of $\tan \theta_x$. The lower bounds on $M_{Z'}$, arising from the ATLAS exclusion of the DY production of Z' , are depicted as the dark red lines, whereas the interiors of the light blue lines denote the region allowed by ν_μ - e scattering data. For both red and blue contours, the dotted and dashed lines correspond to $\tan \theta_x = 1$ and 4 respectively. Recall that $\tan \theta_x$ is proportional to the $U(1)_X$ coupling, g_x . As expected, the bounds become stronger with increasing $\tan \theta_x$. Combining the lower bound on $M_{Z'}$ from the direct searches with the corresponding upper bound

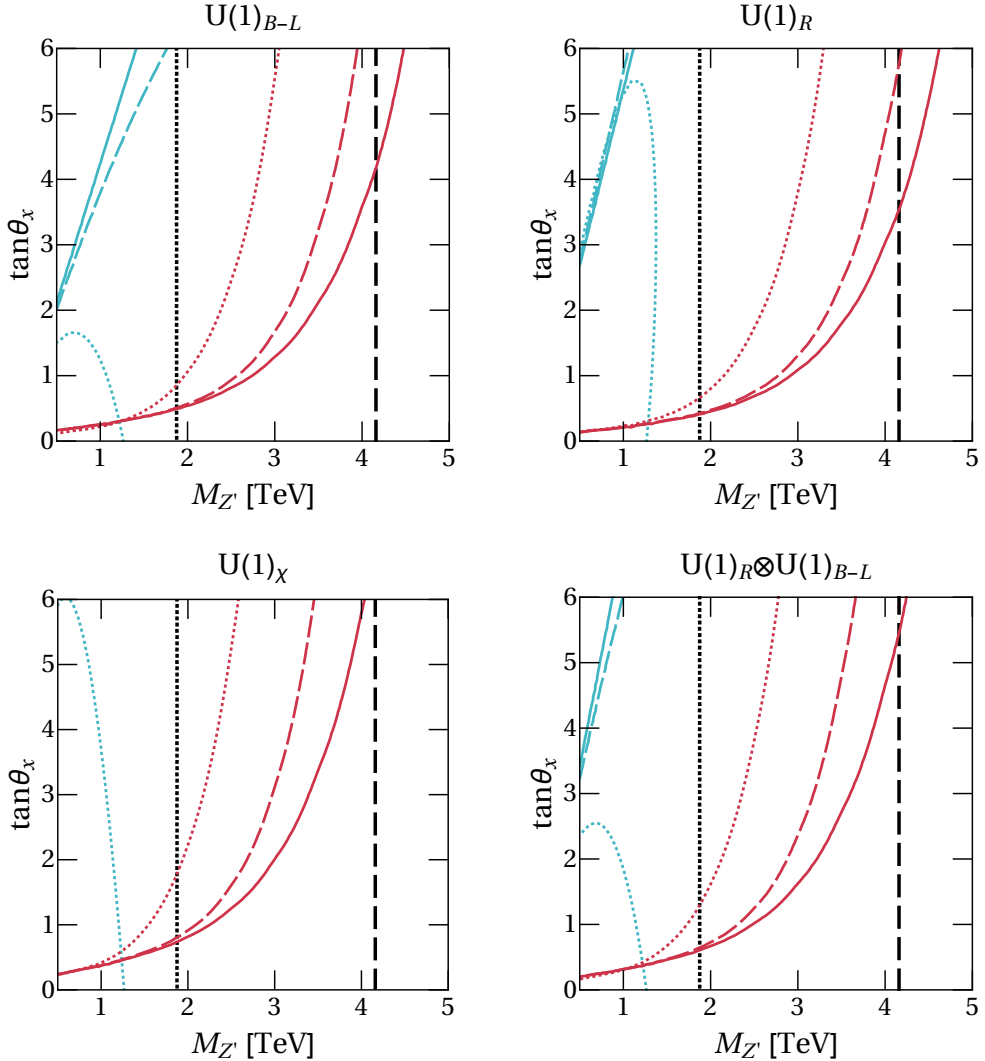


Figure 3: Bounds in the $M_{Z'}$ - $\tan\theta_x$ plane for the four models listed in Table 2. In every panel, the region on the left of the black lines is allowed from unitarity. The dark red and the light blue lines denote the limits set by direct detection and ν_μ - e scattering data, respectively. The dotted, dashed and solid line types correspond to $\sin\alpha_z = 0.01, 0.002$ and 0 , respectively. Regions to the right of the dark red lines are allowed by the 36 fb^{-1} ATLAS data. For the solid and dashed light blue lines, the regions to the right are allowed while for the dotted light blue line the interior region is allowed.

coming from, *e.g.*, unitarity, we are able to extract an upper limit on the magnitude of the Z - Z' mixing angle, α_z . Such bounds on $|\alpha_z|$ are at par with the corresponding limits from electroweak precision data [42–44, 66].

In Table 3, we have summarized the bounds on α_z , and $M_{Z'}$, for $\tan\theta_x=1$ and 4 , for the four different $U(1)_X$ models under consideration. From Table 2 we recall that the choice $\tan\theta_x = 4$ corresponds to $g'_x = g$ for the conventional $(B-L)$ model. In Table 3 we also note that the lower bound on $M_{Z'}$ becomes weaker as the value of α_z deviates from zero. This is because, for non-zero α_z , Z' can decay into W^+W^- , which results in a reduction of the branching ratio of the Z' decaying into two charged leptons [67]. Additionally, it should also be pointed out that although we have taken into account the decays $Z' \rightarrow W^+W^-$ and $Z' \rightarrow Zh$ (h being the lighter SM-like Higgs scalar) for our analysis, we have assumed the decays $Z' \rightarrow NN$, where N denotes a heavy RH neutrino, and $Z' \rightarrow ZH$, where H is the heavier nonstandard scalar, to be kinematically forbidden. The lower bounds on $M_{Z'}$ should be diluted further if these decay channels open up.

In Fig. 3, we take a complementary approach by casting the bounds in the $\tan\theta_x$ - $M_{Z'}$ plane, for three representative values of $\sin\alpha_z$. The color conventions remain the same, *i.e.*, the dark red lines still denote the contours coming from direct searches, while the light blue and the black lines denote the constraints coming from ν_μ - e

⁶For the four models discussed here, we have checked that the constraint from $g_A^{\nu_e}$ is overshadowed by that coming from $g_V^{\nu_e}$.

Model		$U(1)_{B-L}$	$U(1)_{1R}$	$U(1)_X$	$U(1)_R \times U(1)_{B-L}$
$\tan \theta_x = 4$	Maximum $ \sin \alpha_z $	0.003	0.002	0.004	0.003
	$M_{Z'}$ exclusion at $\alpha_z = 0$ [TeV]	4.1	4.3	3.7	3.9
	$M_{Z'}$ exclusion at maximum $ \sin \alpha_z $ [TeV]	3.5	3.8	2.8	3.1
$\tan \theta_x = 1$	Maximum $ \sin \alpha_z $	0.006	0.005	0.008	0.007
	$M_{Z'}$ exclusion at $\alpha_z = 0$ [TeV]	2.8	2.9	2.2	2.6
	$M_{Z'}$ exclusion at maximum $ \sin \alpha_z $ [TeV]	2.2	2.5	1.7	1.9

Table 3: *Bounds on $M_{Z'}$ and α_z for different $U(1)_X$ models for two representative values of $\tan \theta_x$, which is proportional to the $U(1)_X$ coupling.*

scattering and unitarity, respectively. Dotted, dashed, and solid lines correspond to $\sin \alpha_z = 0.01, 0.002$, and 0 respectively. For the black unitarity contours in Fig. 3, the region on the left of the corresponding vertical line is allowed, whereas, for the dark red curves the allowed region is on the right of the corresponding curve. For the solid and dashed light blue curves, the regions to the right are allowed while, for the dotted light blue curve the interior region is allowed. The absence of a certain type of contour in Fig. 3 implies that the corresponding curve is too weak to put any constraints on the chosen range of the parameter space.

7 Conclusions

Our intention in this paper has been to put constraints on the parameter space of the minimal extension of the SM with an additional gauged $U(1)$ giving a massive neutral Z' gauge boson. We did revisit the formalism first to set up the notations. Importantly, we have not *a priori* assumed, unlike most of the previous works, that the Z - Z' mixing angle is small or the Z' mass is way above the Z mass. The possibility of kinetic mixing has also been included in our analysis. We examine several alternative choices of the extra $U(1)$ symmetry, e.g., the $(B-L)$ model, an $U(1)$ arising from left-right symmetry, etc. It turns out that there are three most important quantities which cover the extended parameter space: the mass of the Z' , the effective gauge coupling strength (g'_x) of the extra $U(1)$, and the Z - Z' mixing angle (α_z). To constrain this space, we have primarily employed three types of information, namely, the LHC (ATLAS) 13 TeV Drell-Yan data with 36 fb^{-1} luminosity, the results from low energy $\nu_\mu - e$ scattering, and consistency with s -wave unitarity in the $W_L^+ W_L^- \rightarrow W_L^+ W_L^-$ channel. The highlights of our paper are the following:

- We have updated the model-independent constraints in the $C_u^\ell - C_d^\ell$ ($\ell \equiv e, \mu$) plane, using the latest 13 TeV (36 fb^{-1}) ATLAS data. We obtain an improvement of one order of magnitude over the previous constraints in the same plane obtained from the publicly available 7-8 TeV CMS results [56] (see also [33]), and several orders of magnitude over those from Tevatron results [30]. While constraints were speculated before actual LHC data arrived [10, 31, 32], our analysis provides the most updated ones in the $C_u^\ell - C_d^\ell$ plane using the latest publicly available LHC (ATLAS) data. Translating experimental data to constraints in the above plane as a function of $(M_{Z'}, C_u^\ell, C_d^\ell)$, rather than directly to limits on $M_{Z'}/g_x^2$, is quite useful as it provides a model independent platform from where limits on any type of specific customized models can be easily extracted. ATLAS has also provided bounds for Drell-Yan $\tau^+ \tau^-$ production through a Z' . We use this dataset to set similar constraints in the $C_u^\tau - C_d^\tau$ plane. Though less restrictive, these latter bounds are useful for non-universal Z' models which have a different coupling to the third generation fermions.
- The s -wave unitarity constraints in the $(M_{Z'} - \sin \alpha_z)$ plane, placed for the first time in this paper, turn out to provide complementary limits when the LHC direct search and the low energy $\nu_\mu - e$ scattering constraints are superposed in the same plane. It is important to observe that the unitarity constraints are insensitive to the extra $U(1)$ coupling strength, g'_x , and in conjunction with the LHC direct search limits they restrict the Z - Z' mixing to be small (which we have not *a priori* assumed). It is also noteworthy that the relative importance between the unitarity constraints and the neutrino-electron scattering data depends on the value of g'_x . The constraints on the mixing angle we obtain are, in fact, of the same order as obtained from electroweak precision tests [42–44].
- For a typical choice of $g'_x = g \simeq 0.65$, we obtain $M_{Z'} > 3.5 \text{ TeV}$ and $|\alpha_z| < 0.003$ for the $U(1)_{B-L}$ model, from a combined constraint of 36 fb^{-1} ATLAS data and unitarity constraints. If we assume that the Z - Z' mixing angle is zero, the bound soars up to 4 TeV. For other $U(1)$ scenarios the bounds we obtain are in the same ballpark.

We urge our experimental colleagues to take notice of our analysis.

Note added: While this manuscript was being finalized, the 13 TeV Drell-Yan data from the CMS Collaboration became available [68]. Our result in the $C_u^{e,\mu}-C_d^{e,\mu}$ plane, which uses the 13 TeV ATLAS Drell-Yan data, is very similar to that obtained by the CMS collaboration. Analysis using the 13 TeV ATLAS Drell-Yan data has also been performed very recently in Refs. [69, 70].

Acknowledgements: TB acknowledges a Senior Research Fellowship from UGC, India. GB and AR acknowledge support of the J.C. Bose National Fellowship from the Department of Science and Technology, Government of India (SERB Grant Nos. SB/S2/JCB-062/2016 and SR/S2/JCB-14/2009, respectively). AR also acknowledges support from the SERB Grant No. EMR/2015/001989.

Appendix: Detailed expressions for w_q

The NLO expressions for the functions, w_q , which appear in Eq. (26), are given by

$$w_q(s, M_{Z'}^2) = \int_0^1 dx \int_0^1 dy \int_0^1 dz \delta\left(\frac{M_{Z'}^2}{s} - xyz\right) \times \left\{ F_{qq}(x, y, M_{Z'}^2) \Delta_{qq}(z, M_{Z'}^2) + F_{gq}(x, y, M_{Z'}^2) \Delta_{gq}(z, M_{Z'}^2) \right\}, \quad (\text{A.1})$$

For pp colliders such as the LHC we have [30]:

$$F_{qq}(x, y, M_{Z'}^2) = f_{q\leftarrow P}(x, M_{Z'}^2) f_{\bar{q}\leftarrow P}(y, M_{Z'}^2) + (x \leftrightarrow y), \quad (\text{A.2a})$$

$$F_{gq}(x, y, M_{Z'}^2) = f_{g\leftarrow P}(x, M_{Z'}^2) [f_{q\leftarrow P}(y, M_{Z'}^2) + f_{\bar{q}\leftarrow P}(y, M_{Z'}^2)] + (x \leftrightarrow y), \quad (\text{A.2b})$$

where $f_{q\leftarrow P}(x, M_{Z'}^2)$ represents the PDF for the parton q at a factorization scale, $M_{Z'}$. The scaling functions, Δ_{qq} and Δ_{gq} , are given by [71]

$$\Delta_{qq}(z, M_{Z'}^2) = \delta(1-z) + \frac{\alpha_s(M_{Z'}^2)}{\pi} C_F \left[\left(\frac{\pi^2}{3} - 4 \right) \delta(1-z) - \frac{1+z^2}{1-z} \ln(z) - 2(1+z) \ln(1-z) + 4(1+z^2) \left(\frac{\ln(1-z)}{1-z} \right)_+ \right], \quad (\text{A.3a})$$

$$\Delta_{gq}(z, M_{Z'}^2) = \frac{\alpha_s(M_{Z'}^2)}{2\pi} T_F \left[(1-2z+2z^2) \ln \frac{(1-z)^2}{z} + \frac{1}{2} + 3z - \frac{7}{2} z^2 \right], \quad (\text{A.3b})$$

where $C_F = 4/3$ and $T_F = 1/2$ are the quark and gluon color factors respectively. The plus prescription is defined as follows:

$$\int_0^1 dx f(x) g(x)_+ = \int_0^1 dx [f(x) - f(1)] g(x). \quad (\text{A.4})$$

We obtained our numerical results using these equations.

References

- [1] J. C. Pati and A. Salam, *Is Baryon Number Conserved?*, *Phys. Rev. Lett.* **31** (1973) 661–664.
- [2] J. C. Pati and A. Salam, *Lepton Number as the Fourth Color*, *Phys. Rev.* **D10** (1974) 275–289. [Erratum: *Phys. Rev.* **D11**, 703 (1975)].
- [3] R. N. Mohapatra and J. C. Pati, “*Natural*” *left-right symmetry*, *Phys. Rev.* **D11** (1975) 2558–2561.
- [4] G. Senjanovic and R. N. Mohapatra, *Exact Left-Right Symmetry and Spontaneous Violation of Parity*, *Phys. Rev.* **D12** (1975) 1502–1505.

- [5] H. Georgi, *The State of the Art Gauge Theories*, *AIP Conf.Proc.* **23** (1975) 575–582.
- [6] H. Fritzsch and P. Minkowski, *Unified Interactions of Leptons and Hadrons*, *Annals Phys.* **93** (1975) 193–266.
- [7] F. Gursey, P. Ramond, and P. Sikivie, *A Universal Gauge Theory Model Based on E_6* , *Phys. Lett.* **60B** (1976) 177–180.
- [8] D. London and J. L. Rosner, *Extra Gauge Bosons in $E(6)$* , *Phys. Rev.* **D34** (1986) 1530.
- [9] P. Langacker, *Grand Unified Theories and Proton Decay*, *Phys. Rept.* **72** (1981) 185.
- [10] T. G. Rizzo, *Z' phenomenology and the LHC*, in *Proceedings of Theoretical Advanced Study Institute in Elementary Particle Physics : Exploring New Frontiers Using Colliders and Neutrinos (TASI 2006): Boulder, Colorado, June 4-30, 2006*, pp. 537–575, 2006. [hep-ph/0610104](#).
- [11] J. L. Hewett and T. G. Rizzo, *Low-Energy Phenomenology of Superstring Inspired $E(6)$ Models*, *Phys. Rept.* **183** (1989) 193.
- [12] M. Cvetič and P. Langacker, *Implications of Abelian extended gauge structures from string models*, *Phys. Rev.* **D54** (1996) 3570–3579, [[hep-ph/9511378](#)].
- [13] A. Leike, *The Phenomenology of extra neutral gauge bosons*, *Phys. Rept.* **317** (1999) 143–250, [[hep-ph/9805494](#)].
- [14] P. Langacker, *The Physics of Heavy Z' Gauge Bosons*, *Rev. Mod. Phys.* **81** (2009) 1199–1228, [[arXiv:0801.1345](#)].
- [15] N. Arkani-Hamed, A. G. Cohen, and H. Georgi, *Electroweak symmetry breaking from dimensional deconstruction*, *Phys. Lett.* **B513** (2001) 232–240, [[hep-ph/0105239](#)].
- [16] M. Perelstein, *Little Higgs models and their phenomenology*, *Prog. Part. Nucl. Phys.* **58** (2007) 247–291, [[hep-ph/0512128](#)].
- [17] Y. Shadmi and Y. Shirman, *Dynamical supersymmetry breaking*, *Rev. Mod. Phys.* **72** (2000) 25–64, [[hep-th/9907225](#)].
- [18] I. Antoniadis, *A Possible new dimension at a few TeV*, *Phys. Lett.* **B246** (1990) 377–384.
- [19] T. Appelquist, H.-C. Cheng, and B. A. Dobrescu, *Bounds on universal extra dimensions*, *Phys. Rev.* **D64** (2001) 035002, [[hep-ph/0012100](#)].
- [20] K. Agashe, A. Delgado, M. J. May, and R. Sundrum, *$RS1$, custodial isospin and precision tests*, *JHEP* **08** (2003) 050, [[hep-ph/0308036](#)].
- [21] S. Iso, N. Okada, and Y. Orikasa, *The minimal $B-L$ model naturally realized at TeV scale*, *Phys. Rev.* **D80** (2009) 115007, [[arXiv:0909.0128](#)].
- [22] S. Oda, N. Okada, D. Raut, and D.-s. Takahashi, *Non-minimal quartic inflation in classically conformal $U(1)_X$ extended Standard Model*, [arXiv:1711.09850](#).
- [23] A. Achúcarro and T. Vachaspati, *Semilocal and electroweak strings*, *Phys. Rept.* **327** (2000) 347–426, [[hep-ph/9904229](#)]. [*Phys. Rept.* 327,427(2000)].
- [24] E. Dudas, Y. Mambrini, S. Pokorski, and A. Romagnoni, *(In)visible Z -prime and dark matter*, *JHEP* **08** (2009) 014, [[arXiv:0904.1745](#)].
- [25] E. Dudas, Y. Mambrini, S. Pokorski, and A. Romagnoni, *Extra $U(1)$ as natural source of a monochromatic gamma ray line*, *JHEP* **10** (2012) 123, [[arXiv:1205.1520](#)].
- [26] S. Okada, *Z' portal dark matter in the minimal $B - L$ model*, [arXiv:1803.06793](#).
- [27] B. Kors and P. Nath, *A Stueckelberg extension of the standard model*, *Phys. Lett.* **B586** (2004) 366–372, [[hep-ph/0402047](#)].
- [28] A. Berlin, D. Hooper, and S. D. McDermott, *Simplified Dark Matter Models for the Galactic Center Gamma-Ray Excess*, *Phys. Rev.* **D89** (2014), no. 11 115022, [[arXiv:1404.0022](#)].

- [29] J. M. Cline, G. Dupuis, Z. Liu, and W. Xue, *The windows for kinetically mixed Z' -mediated dark matter and the galactic center gamma ray excess*, *JHEP* **08** (2014) 131, [[arXiv:1405.7691](#)].
- [30] M. Carena, A. Daleo, B. A. Dobrescu, and T. M. P. Tait, *Z' gauge bosons at the Tevatron*, *Phys. Rev.* **D70** (2004) 093009, [[hep-ph/0408098](#)].
- [31] F. Petriello and S. Quackenbush, *Measuring Z' couplings at the CERN LHC*, *Phys. Rev.* **D77** (2008) 115004, [[arXiv:0801.4389](#)].
- [32] E. Salvioni, G. Villadoro, and F. Zwirner, *Minimal Z' -prime models: Present bounds and early LHC reach*, *JHEP* **11** (2009) 068, [[arXiv:0909.1320](#)].
- [33] E. Accomando, A. Belyaev, L. Fedeli, S. F. King, and C. Shepherd-Themistocleous, *Z' physics with early LHC data*, *Phys. Rev.* **D83** (2011) 075012, [[arXiv:1010.6058](#)].
- [34] M. R. Buckley, D. Hooper, J. Kopp, and E. Neil, *Light Z' Bosons at the Tevatron*, *Phys. Rev.* **D83** (2011) 115013, [[arXiv:1103.6035](#)].
- [35] E. Accomando, C. Coriano, L. Delle Rose, J. Fiaschi, C. Marzo, and S. Moretti, *Z , Higgses and heavy neutrinos in $U(1)$ models: from the LHC to the GUT scale*, *JHEP* **07** (2016) 086, [[arXiv:1605.02910](#)].
- [36] N. Okada and S. Okada, *Z'_{BL} portal dark matter and LHC Run-2 results*, *Phys. Rev.* **D93** (2016), no. 7 075003, [[arXiv:1601.07526](#)].
- [37] A. De Simone, G. F. Giudice, and A. Strumia, *Benchmarks for Dark Matter Searches at the LHC*, *JHEP* **06** (2014) 081, [[arXiv:1402.6287](#)].
- [38] O. Buchmueller, M. J. Dolan, S. A. Malik, and C. McCabe, *Characterising dark matter searches at colliders and direct detection experiments: Vector mediators*, *JHEP* **01** (2015) 037, [[arXiv:1407.8257](#)].
- [39] O. Ducu, L. Heurtier, and J. Maurer, *LHC signatures of a Z' mediator between dark matter and the $SU(3)$ sector*, *JHEP* **03** (2016) 006, [[arXiv:1509.05615](#)].
- [40] R. Gauld, F. Goertz, and U. Haisch, *On minimal Z' explanations of the $B \rightarrow K^* \mu^+ \mu^-$ anomaly*, *Phys. Rev.* **D89** (2014) 015005, [[arXiv:1308.1959](#)].
- [41] A. J. Buras and J. Girrbach, *Left-handed Z' and Z FCNC quark couplings facing new $b \rightarrow s \mu^+ \mu^-$ data*, *JHEP* **12** (2013) 009, [[arXiv:1309.2466](#)].
- [42] J. Erler, P. Langacker, S. Munir, and E. Rojas, *Improved Constraints on Z' -prime Bosons from Electroweak Precision Data*, *JHEP* **08** (2009) 017, [[arXiv:0906.2435](#)].
- [43] G. Bhattacharyya, A. Datta, S. N. Ganguli, and A. Raychaudhuri, *Z - Z' -prime mixing in extended gauge models from LEP 1990 data*, *Mod. Phys. Lett.* **A6** (1991) 2557–2568.
- [44] G. Bhattacharyya, A. Raychaudhuri, A. Datta, and S. N. Ganguli, *Z DECAY CONFRONTS NONSTANDARD SCENARIOS*, *Phys. Rev. Lett.* **64** (1990) 2870–2873.
- [45] R. H. Benavides, L. Muoz, W. A. Ponce, O. Rodriguez, and E. Rojas, *Electroweak couplings and LHC constraints on alternative Z' models in E_6* , [[arXiv:1801.10595](#)].
- [46] A. Ekstedt, R. Enberg, G. Ingelman, J. Lfgren, and T. Mandal, *Constraining minimal anomaly free $U(1)$ extensions of the Standard Model*, *JHEP* **11** (2016) 071, [[arXiv:1605.04855](#)].
- [47] **ATLAS** Collaboration, M. Aaboud et al., *Search for new high-mass phenomena in the dilepton final state using 36 fb^1 of proton-proton collision data at $\sqrt{s} = 13 \text{ TeV}$ with the ATLAS detector*, *JHEP* **10** (2017) 182, [[arXiv:1707.02424](#)].
- [48] **ATLAS** Collaboration, M. Aaboud et al., *Search for additional heavy neutral Higgs and gauge bosons in the ditau final state produced in 36 fb^1 of pp collisions at $\sqrt{s} = 13 \text{ TeV}$ with the ATLAS detector*, *JHEP* **01** (2018) 055, [[arXiv:1709.07242](#)].
- [49] B. Holdom, *Two $U(1)$'s and Epsilon Charge Shifts*, *Phys. Lett.* **166B** (1986) 196–198.
- [50] K. S. Babu, C. F. Kolda, and J. March-Russell, *Implications of generalized Z - Z' -prime mixing*, *Phys. Rev.* **D57** (1998) 6788–6792, [[hep-ph/9710441](#)].

- [51] B. Brahmachari and A. Raychaudhuri, *Perturbative generation of θ_{13} from tribimaximal neutrino mixing*, *Phys. Rev.* **D86** (2012) 051302, [[arXiv:1204.5619](#)].
- [52] D. Feldman, Z. Liu, and P. Nath, *The Stueckelberg Z Prime at the LHC: Discovery Potential, Signature Spaces and Model Discrimination*, *JHEP* **11** (2006) 007, [[hep-ph/0606294](#)].
- [53] G. Paz and J. Roy, *A comment on the Z' Drell-Yan cross section*, [arXiv:1711.02655](#).
- [54] A. A. Andrianov, P. Osland, A. A. Pankov, N. V. Romanenko, and J. Sirkka, *On the phenomenology of a Z' coupling only to third family fermions*, *Phys. Rev.* **D58** (1998) 075001, [[hep-ph/9804389](#)].
- [55] S. Dulat, T.-J. Hou, J. Gao, M. Guzzi, J. Huston, P. Nadolsky, J. Pumplin, C. Schmidt, D. Stump, and C. P. Yuan, *New parton distribution functions from a global analysis of quantum chromodynamics*, *Phys. Rev.* **D93** (2016), no. 3 033006, [[arXiv:1506.07443](#)].
- [56] **CMS Collaboration**, V. Khachatryan et al., *Search for physics beyond the standard model in dilepton mass spectra in proton-proton collisions at $\sqrt{s} = 8$ TeV*, *JHEP* **04** (2015) 025, [[arXiv:1412.6302](#)].
- [57] D. J. Muller and S. Nandi, *Top flavor: A Separate $SU(2)$ for the third family*, *Phys. Lett.* **B383** (1996) 345–350, [[hep-ph/9602390](#)].
- [58] K. R. Lynch, E. H. Simmons, M. Narain, and S. Mrenna, *Finding Z' bosons coupled preferentially to the third family at LEP and the Tevatron*, *Phys. Rev.* **D63** (2001) 035006, [[hep-ph/0007286](#)].
- [59] R. Benavides, L. A. Muoz, W. A. Ponce, O. Rodriguez, and E. Rojas, *Minimal nonuniversal electroweak extensions of the standard model: A chiral multiparameter solution*, *Phys. Rev.* **D95** (2017), no. 11 115018, [[arXiv:1612.07660](#)].
- [60] G. Bhattacharyya, D. Das, and P. B. Pal, *Modified Higgs couplings and unitarity violation*, *Phys. Rev.* **D87** (2013) 011702, [[arXiv:1212.4651](#)].
- [61] K. S. Babu, J. Julio, and Y. Zhang, *Perturbative unitarity constraints on general W' models and collider implications*, *Nucl. Phys.* **B858** (2012) 468–487, [[arXiv:1111.5021](#)].
- [62] K. Cheung, C.-W. Chiang, Y.-K. Hsiao, and T.-C. Yuan, *Longitudinal Weak Gauge Bosons Scattering in Hidden Z -prime Models*, *Phys. Rev.* **D81** (2010) 053001, [[arXiv:0911.0734](#)].
- [63] M. Lindner, F. S. Queiroz, W. Rodejohann, and X.-J. Xu, *Neutrino-Electron Scattering: General Constraints on Z' and Dark Photon Models*, [arXiv:1803.00060](#).
- [64] M. Abdullah, J. B. Dent, B. Dutta, G. L. Kane, S. Liao, and L. E. Strigari, *Coherent Elastic Neutrino Nucleus Scattering (CEvNS) as a probe of Z' through kinetic and mass mixing effects*, [arXiv:1803.01224](#).
- [65] **Particle Data Group Collaboration**, C. Patrignani et al., *Review of Particle Physics*, *Chin. Phys.* **C40** (2016), no. 10 100001.
- [66] M. Czakon, J. Gluza, F. Jegerlehner, and M. Zralek, *Confronting electroweak precision measurements with new physics models*, *Eur. Phys. J.* **C13** (2000) 275–281, [[hep-ph/9909242](#)].
- [67] P. Osland, A. A. Pankov, and A. V. Tsytrinov, *Probing Z - Z' mixing with ATLAS and CMS resonant diboson production data at the LHC at $\sqrt{s} = 13$ TeV*, *Phys. Rev.* **D96** (2017), no. 5 055040, [[arXiv:1707.02717](#)].
- [68] **CMS Collaboration**, A. M. Sirunyan et al., *Search for high-mass resonances in dilepton final states in proton-proton collisions at $\sqrt{s} = 13$ TeV*, [arXiv:1803.06292](#).
- [69] A. Gulov, A. Pankov, A. Pevzner, and V. Skalozub, *Model-independent constraints on the Abelian Z' couplings within the ATLAS data on the dilepton production processes at $\sqrt{s} = 13$ TeV*, [arXiv:1803.07532](#).
- [70] A. Pevzner, *Influence of the $Z - Z'$ mixing on the Z' production cross section in the model-independent approach*, [arXiv:1803.07508](#).
- [71] R. Hamberg, W. L. van Neerven, and T. Matsuura, *A complete calculation of the order $\alpha - s^2$ correction to the Drell-Yan K factor*, *Nucl. Phys.* **B359** (1991) 343–405. [Erratum: *Nucl. Phys.*B644,403(2002)].